

Membrane Phenomena in Nonisothermal Systems: Part 2. Effect of Hydrophobicity of Ion-Exchange Groups of Anion-Exchange Membranes on Thermoosmosis

Ryotaro Kiyono,* Atsuhito Komoto, Masayasu Tasaka, Takanori Yamaguchi,[†] and Toshikatsu Sata[†]

Department of Chemistry and Material Engineering, Faculty of Engineering, Shinshu University, Wakasato, Nagano 380

[†]Department of Applied Chemistry and Chemical Engineering, Faculty of Engineering, Yamaguchi University, Tokiwadai, Ube, Yamaguchi 755

(Received December 4, 1996)

Solvent transport across poly(styrene)-based anion-exchange membranes with various ion-exchange groups was measured under a temperature gradient to discuss the effect of hydrophobicity of the membranes on thermoosmosis. Two varieties of poly(styrene)-based copolymer membranes with 10 and 14% divinylbenzene as cross-linking agent were prepared as base membranes. Benzyltrimethylammonium, benzyltriethylammonium, benzyltripropylammonium, benzyltributylammonium, and benzyltripentylammonium were introduced in the base membranes as anion-exchange groups. The thermoosmotic volume flux toward the hot solution side decreased with increasing the length of alkyl groups (increasing hydrophobicity of the groups), and at last, for the membranes with benzyltripentylammonium, the direction of thermoosmosis reversed: from the hot to the cold solution side as is observed for usual hydrophobic membranes. The transported energy and the mean transported entropy of water in the membranes estimated from the data of thermoosmosis and that of osmosis measurements increased with increasing the hydrophobicity of the ion-exchange groups introduced in the membranes.

For anion-exchange membranes, in general, the direction of thermoosmosis has been observed from the cold solution side to the hot solution side.^{1,2)} Recently, however, for weak-base anion-exchange membranes containing poly(4-vinylpyridine) or poly(*N*-vinyl-2-methylimidazole), which are expected to act as hydrophobic membranes, thermoosmosis toward the cold solution side was observed, because the entropy of water in the membrane is higher than that of the external solution phase due to the high hydrophobicity in the membranes.³⁾ Actually for sulfonic acid-type cation-exchange membrane with the alkylammonium ion forms: $(C_2H_5)_4N^+$, $(n-C_3H_7)_4N^+$, and $(n-C_4H_9)_4N^+$, the thermoosmotic volume flux toward the hot solution side decreased with increasing the hydrophobicity of the counterions, and at last, for the membranes with the higher hydrophobic ion forms, the direction of thermoosmosis reversed: from the hot to the cold solution side.⁴⁾ Therefore, even for strong-base anion-exchange membranes, if the hydrophobicity of the membranes is very much higher, it may be expected that the direction of thermoosmosis reversed from the hot solution side to the cold side.

In this study we planned to prepare a series of membranes having various types of hydrophobicity by changing the length of the alkyl chains of the amines as anion-exchange groups. Two varieties of poly(styrene)-based copolymer membranes with 10 and 14% divinylbenzene were prepared as base membranes. Five trialkylbenzylammonium groups with different lengths of alkyl chains: benzyltrimethylammonium, benzyltriethylammonium, benzyltripropylammo-

nium, benzyltributylammonium, and benzyltripentylammonium, were introduced in the base membranes as anion-exchange groups. We measured solvent transport across these anion-exchange membranes with various ionic groups under a temperature gradient and discussed the effect of hydrophobicity of the membranes on thermoosmosis. The transported energy and the mean transported entropy of water in the membranes were estimated after combining the data of thermoosmosis and that of osmosis measurements.

Experimental

Membranes and Electrolytes. Two varieties of poly(styrene)-based copolymer membranes with 10 and 14% divinylbenzene as cross-linking agent, M(10) and M(14), were prepared as base membranes. After polymerization, the obtained copolymer membrane reacted with amines: an aqueous 1 mol dm⁻³ trimethylamine solution for M-1; 1 mol dm⁻³ triethylamine, tripropylamine, and tributylamine methyl alcohol solutions for M-2, M-3, and M-4, respectively; and a 1 mol dm⁻³ tripentylamine ethyl alcohol solution for M-5. Other details for the preparation of the membranes were reported elsewhere.⁵⁾ Ion-exchange capacity of the membranes was measured using the gravimetric method,⁶⁾ and expressed by the unit mmol of ion-exchange groups per gram of the dry membranes without the weight of anhydrous counterions. Water content of the membranes was measured carefully using the same method as that reported in a previous paper.⁷⁾ The water content was expressed by the unit: grams of water per gram of the dry membranes without the weight of anhydrous counterions.

The reagents used for the preparation of aqueous KCl and KIO₃ solutions were special grades from Wako Pure Chemical Industries,

Ltd.

Measurements of Thermoosmosis. Thermoosmotic volume flux was measured using the same apparatus as that used in the previous paper.¹⁾ The cell for the measurement of thermoosmosis consisted of two chambers separated by a horizontal membrane. The upper 1500 cm³ hot chamber was separated from the lower 96 cm³ cold chamber by a membrane. The effective area of the membrane was 28 cm². The mean temperature of the two chambers were fixed at 308.2 K throughout the measurements. The ratio of effective temperature difference across the membrane, ΔT , to the temperature difference of two bulk solution, ΔT_b , was about 0.7.¹⁾ The molalities of the external solution were 0.01 mol kg⁻¹.

Measurements of Osmotic Volume Flux. Osmotic volume flux under a concentration gradient was measured using the same cell as that used in the previous paper.²⁾ The membrane was mounted between two 65 cm³ PVC half cells. The effective membrane area was 2.54 cm². The osmotic pressure difference was applied using sucrose solutions with different concentrations.

Results and Discussion

The thickness, ion-exchange capacity, water content for the Cl⁻ and IO₃⁻ forms of the membranes, and transport number of Cl⁻, are summarized in Table 1. The ion-exchange capacity and water content of the membranes decreased as a whole with increasing the chain length of alkyl groups of trialkylbenzylammonium. But, water contents of M-2(10) and M-2(14) were almost equal to or a little larger than those of M-1(10) and M-1(14), respectively. When the base copolymer membranes were reacted with amines for quaternization, the base membrane was immersed in an aqueous trimethylamine solution for the preparation of the membrane M-1, while the membranes M-2 to M-5 were immersed in trialkylamine methyl or ethyl alcohol solutions, as mentioned in the Experimental section. The smaller water content of M-1 compared with that of M-2 would be due to the difference in solvent for the quaternization. In general, the hydrophobicity of the membranes increased with increasing the length of alkyl chains of trialkylammonium groups. The ion-exchange capacity and water content for the series of the membranes M(14) were a little smaller than those for the series of the membranes M(10) because the DVB content of

M(14) was larger than that of M(10). The water contents of the membranes with the IO₃⁻ forms were higher than those with the Cl⁻ forms. This is because the hydration of IO₃⁻ ions is larger than that of Cl⁻ ions. The transport numbers of anions estimated from the concentration membrane potential in 0.03/0.06 mol kg⁻¹ of KCl solution systems were 1.00 for all membranes, as shown in Table 1. Therefore, these membranes can be considered to be ideally perm-selective for counterions under the experimental conditions.

If anion-exchange membranes have ideal perm-selectivity for counterions, the volume flux, J_v , across the membranes due to a logarithmic temperature difference, $\Delta \ln T$, and an osmotic pressure difference, $\Delta \pi$, can be written as⁸⁾

$$\begin{aligned} -J_v &= D^* [(\bar{e}_0 - s_0 T_m) \Delta \ln T - v_0 \Delta \pi] \\ &= D^* [(\bar{s}_0 - s_0) T_m \Delta \ln T - v_0 \Delta \pi] \end{aligned} \quad (1)$$

where

$$D^* = (1/\delta)(\bar{c}_0 l_{v0} + \tau_0 F \phi X l_{v-}) \quad (2)$$

Here, the subscripts 0 and - refer to water and anions, \bar{e}_0 is the transported energy per mole of water in the membrane, s_0 the partial molar entropy of water in the external solution, \bar{s}_0 the mean transported entropy of water in the membrane, v_0 the partial molar volume, T_m the mean temperature, \bar{c}_0 the concentration of water in the membrane, τ_0 the reduced transport number of water, δ the thickness of the membrane, F the Faraday constant, and ϕX is the effective concentration of membrane fixed charges. Moreover, the l_{v0} is a parameter related to the mobility of water in the membrane and l_{v-} is related to the interaction between the anions and water. If there is no osmotic pressure difference, Eq. 1 becomes

$$-J_v = D^e \Delta \ln T, \quad D^e = (\bar{e}_0 - s_0 T_m) D^* = (\bar{s}_0 - s_0) T_m D^* \quad (3)$$

Since the state of water is unstable and the energy level of water is high in the hydrophobic membrane, in general, the difference between the transported energy in the membrane and partial molar entropy of water in the external solution multiplied by mean temperature, $(\bar{e}_0 - s_0 T_m)$, or the mean transported entropy of water in the membrane and the partial

Table 1. Properties of Membranes

Membrane ^{a)}	Ion-exchange groups	Thickness mm	Ion-exchange capacity ^{b)}	Water content ^{c)}		Molality of the fixed charges ^{d)}	Transport number of Cl ⁻ ^{e)}
				Cl ⁻ form	IO ₃ ⁻ form		
M-1(10)	Benzyltrimethyl	0.13	2.04	0.32	0.39	6.27	1.00
M-2(10)	Benzyltriethyl	0.13	1.48	0.36	0.43	4.12	1.00
M-3(10)	Benzyltripropyl	0.13	1.20	0.32	0.37	3.70	1.00
M-4(10)	Benzyltributyl	0.13	1.01	0.25	0.31	4.01	1.00
M-5(10)	Benzyltripentyl	0.13	0.87	0.15	0.25	5.79	1.00
M-1(14)	Benzyltrimethyl	0.12	1.84	0.27	0.32	6.70	1.00
M-2(14)	Benzyltriethyl	0.12	1.20	0.27	0.31	4.45	1.00
M-3(14)	Benzyltripropyl	0.12	0.95	0.23	0.25	4.16	1.00
M-4(14)	Benzyltributyl	0.12	0.84	0.17	0.20	4.99	1.00
M-5(14)	Benzyltripentyl	0.12	0.75	0.12	0.14	6.34	1.00

a) Number in parentheses represents the content of divinylbenzene in % b) mmol per g-dry membrane without counterions c) g-H₂O per g-dry membrane without counterions. d) mmol per g-H₂O for the Cl⁻ forms e) Estimated from the concentration membrane potential in 0.03/0.06 mol kg⁻¹ KCl solutions.

molar entropy of water in the external solution, $(\bar{s}_0 - s_0)$, becomes positive, and thermoosmosis occurs from the hot to the cold solution side. On the other hand, as is expected from Eq. 3, if the mean transported entropy of water in the membrane is lower than the partial molar entropy of water in the external solution, as in the case of strong-base anion-exchange membranes, the value of $(\bar{s}_0 - s_0)$ or $(\bar{e}_0 - s_0 T_m)$ is negative, and thermoosmosis occurs toward the hot solution side. Thus, the direction of thermoosmosis depends on the energy difference or the entropy difference of water between in the membrane phase and in the external solution phase.

If there is no temperature difference, Eq. 1 becomes

$$-J_v = L_p \Delta \pi, \quad L_p = -v_0 D^* \quad (4)$$

From the values of D^e and D^* , we can estimate the values of $(\bar{e}_0 - s_0 T_m)$ and $(\bar{s}_0 - s_0)$:

$$(\bar{e}_0 - s_0 T_m) = (\bar{s}_0 - s_0) T_m = D^e / D^* = -v_0 D^e / L_p \quad (5)$$

In Fig. 1, the thermoosmotic volume flux, J_v , across a series of membranes with 10% DVB, M-1(10)—M-5(10), with the Cl^- and the IO_3^- forms were plotted against the logarithmic temperature difference of bulk solutions, $\Delta \ln T_b$. The thermoosmotic coefficient, D^e , were calculated from the linear relationships between J_v and $\Delta \ln T_b$, and values are listed in Tables 2 and 3. The positive sign of the value of $-D^e$ means that the direction of thermoosmosis is from the cold to the hot solution side. For the membranes M-1(10)—M-4(10), thermoosmosis occurred from the cold to the hot solution side, as is observed for usual anion-exchange membranes. However, in general, the magnitude of the flux decreased with increasing the length of alkyl chains of the fixed charge groups, and, at last, for the membrane M-5(10), the direction of thermoosmosis reversed: from the hot side to the cold side, as is observed for hydrophobic membranes. The value of $-D^e$ for M-1(10) with the Cl^- form was smaller than that for M-2(10) with the Cl^- form. As is expected from Eq. 2, the magnitude of the thermoosmotic volume flux is affected more or less by the water content of the membranes, \bar{e}_0 . The smaller value of $-D^e$ for M-1(10), compared with that for M-2(10) with the Cl^- forms, would be due to the smaller

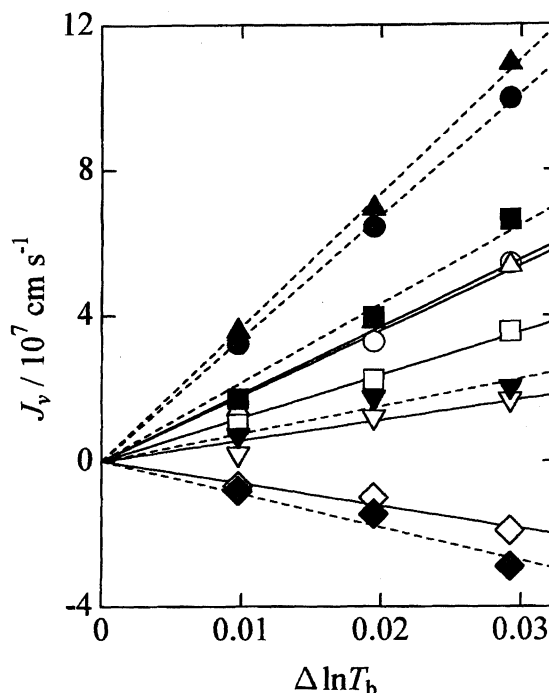


Fig. 1. The thermoosmotic volume flux, J_v , across M-1(10)—M-5(10) for Cl^- forms (open symbol) and IO_3^- forms (filled symbol) plotted against the logarithmic temperature difference of bulk solutions, $\Delta \ln T_b$. Membranes: (○, ●), M-1(10); (△, ▲), M-2(10); (□, ■), M-3(10); (▽, ▼), M-4(10); (◇, ◆), M-5(10).

water content of M-1(10) compared with that of M-2(10). The absolute values of thermoosmosis for the membranes with the IO_3^- forms were always larger than those with the Cl^- forms. These results were attributed to the larger water content of the membranes with the IO_3^- forms compared with that with the Cl^- forms. The relationship between thermoosmotic volume flux, J_v , and $\Delta \ln T_b$ across membranes M-1(14)—M-5(14) are shown in Fig. 2. Similar relationships to that observed for the membranes M(10) were obtained; however, the direction of thermoosmosis had turned toward the cold solution side already for the membrane M-4(14). As mentioned above, the ion-exchange capacity and water

Table 2. Values of $-D^e$, D^* , $\bar{e}_0 - s_0 T_m$, $\bar{s}_0 - s_0$, \bar{e}_0 , and \bar{s}_0 for the Membranes with the Cl^- Forms

Membr.	$-D^e$ $10^{-5} \text{ cm s}^{-1}$	D^* $10^{-8} \text{ cm mol J}^{-1} \text{ s}^{-1}$	$\bar{e}_0 - s_0 T_m$ 10^2 J mol^{-1}	$\bar{s}_0 - s_0$ $\text{J K}^{-1} \text{ mol}^{-1}$	$\bar{e}_0^{\text{a)}$ 10^3 J mol^{-1}	$\bar{s}_0^{\text{a)}$ $\text{J K}^{-1} \text{ mol}^{-1}$
M-1(10)	2.56	10.21	-2.51	-0.81	1.01	3.3
M-2(10)	2.64	11.83	-2.23	-0.72	1.04	3.4
M-3(10)	1.59	7.60	-2.09	-0.68	1.05	3.4
M-4(10)	0.80	5.28	-1.51	-0.49	1.11	3.6
M-5(10)	-0.88	1.63	5.40	1.76	1.80	5.9
M-1(14)	2.10	7.08	-2.97	-0.96	0.97	3.1
M-2(14)	1.62	6.99	-2.32	-0.75	1.03	3.4
M-3(14)	0.90	3.87	-2.33	-0.75	1.03	3.4
M-4(14)	-0.44	2.85	1.54	0.50	1.42	4.6
M-5(14)	-1.99	2.88	6.91	2.25	1.95	6.4

a) Assumed $s_0 = 4.1 \text{ J K}^{-1} \text{ mol}^{-1}$ at 308.2 K.

Table 3. Values of $-D^e$, D^* , $\bar{e}_0 - s_0 T_m$, $\bar{s}_0 - s_0$, \bar{e}_0 , and \bar{s}_0 for the Membranes with the IO_3^- Forms

Membr.	$-D^e$	D^*	$\bar{e}_0 - s_0 T_m$	$\bar{s}_0 - s_0$	\bar{e}_0^{a}	\bar{s}_0^{a}
	$10^{-5} \text{ cm s}^{-1}$	$10^{-8} \text{ cm mol J}^{-1} \text{ s}^{-1}$	10^2 J mol^{-1}	$\text{J K}^{-1} \text{ mol}^{-1}$	10^2 J mol^{-1}	$\text{J K}^{-1} \text{ mol}^{-1}$
M-1(10)	4.82	7.62	-6.3	-2.05	6.3	2.1
M-2(10)	5.25	8.69	-6.0	-1.96	6.6	2.1
M-3(10)	3.08	7.39	-4.1	-1.35	8.5	2.8
M-4(10)	1.08	5.56	-1.9	-0.63	10.7	3.5
M-5(10)	-1.30	3.06	4.3	1.38	16.9	5.5
M-1(14)	3.13	5.84	-5.4	-1.74	7.3	2.4
M-2(14)	2.64	6.51	-4.1	-1.31	8.6	2.8
M-3(14)	2.07	4.06	-5.1	-1.65	7.5	2.5
M-4(14)	-2.77	2.74	10.1	3.28	22.7	7.4
M-5(14)	-3.05	2.99	10.2	3.31	22.8	7.4

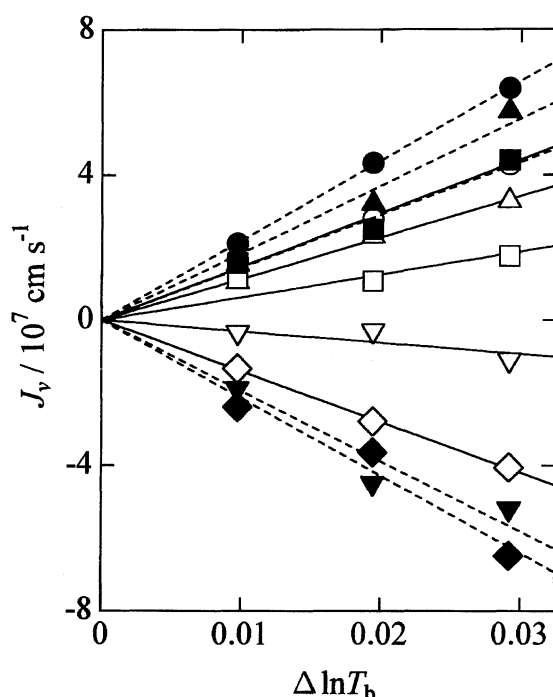
a) Assumed $s_0 = 4.1 \text{ J K}^{-1} \text{ mol}^{-1}$ at 308.2 K.

Fig. 2. The thermoosmotic volume flux, J_v , across M-1(14)—M-5(14) for Cl^- forms (open symbol) and IO_3^- forms (smeared symbol) plotted against the logarithmic temperature difference of bulk solutions, $\Delta \ln T_b$. Membranes: (○, ●), M-1(14); (△, ▲), M-2(14); (□, ■), M-3(14); (▽, ▼), M-4(14); (◇, ◆), M-5(14).

content for the series of the membranes M(14) were a little smaller than those for the series of the membranes M(10) because the DVB content of M(14) was larger than that of M(10). In other words, the series of the membranes M(14) is more hydrophobic than M(10). From these results, it may be concluded that the thermoosmotic volume flux toward the hot solution side decreases with increasing the hydrophobicity of the anion-exchange membranes, and finally, the direction of thermoosmosis turns toward the cold solution side for the more hydrophobic anion-exchange membranes.

Figures 3 and 4 show examples of the relationships between the osmotic volume flux, J_v , and the osmotic pressure

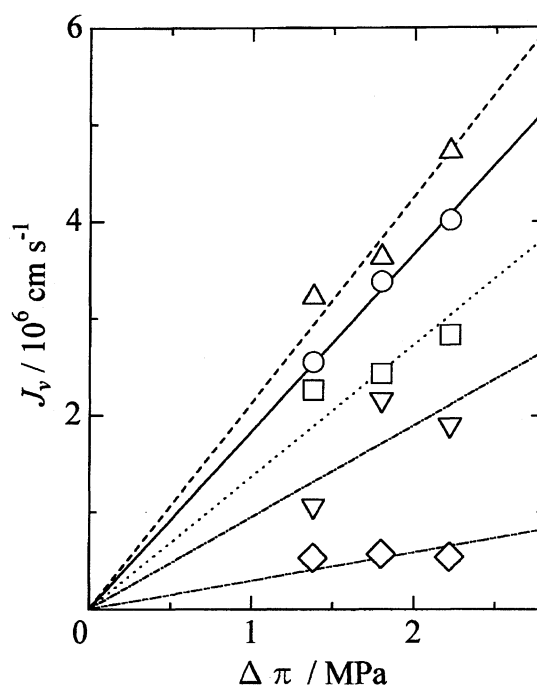


Fig. 3. The relationship between osmotic volume flux, J_v , and osmotic pressure difference, $\Delta \pi$, for membranes M-1(10)—M-5(10) with Cl^- forms. Membranes: (○), M-1(10); (△), M-2(10); (□), M-3(10); (▽), M-4(10); (◇), M-5(10).

difference, $\Delta \pi$, for the membranes M-1(10)—M-5(10) with the Cl^- forms and for the membranes M-1(10)—M-5(10) with the IO_3^- forms, respectively. Linear relationships between J_v and $\Delta \pi$ were observed. The osmotic coefficients, D^* , were calculated from the slopes of these figures and values are listed in Tables 2 and 3. The order of the magnitude of the values of D^* was almost consistent with that of the water content of the membrane. Similar relationships were observed between J_v and $\Delta \pi$ for the membranes M-1(14)—M-5(14).

The values of the energy difference of water between the membrane phase and the external solution phase, $(\bar{e}_0 - s_0 T_m)$, were estimated from the data of D^e and D^* using Eq. 5 and

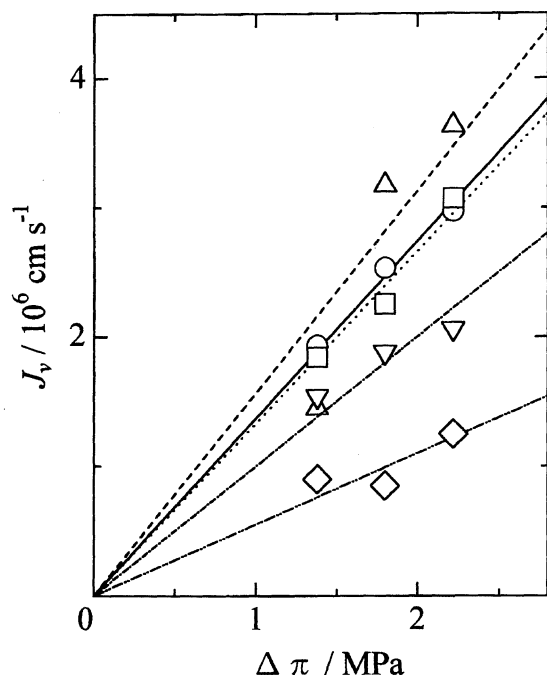


Fig. 4. The relationship between osmotic volume flux, J_v , and osmotic pressure difference, $\Delta\pi$, for membranes M-1(10)—M-5(10) with IO_3^- forms. Membranes: (○), M-1(10); (△), M-2(10); (□), M-3(10); (▽), M-4(10); (◇), M-5(10).

are listed in Tables 2 and 3. The values of $(\bar{s}_0 - s_0)$ can be estimated from the values of $(\bar{e}_0 - s_0 T_m)$ divided by T_m : $(\bar{e}_0 - s_0 T_m)/T_m$; they are also listed in the tables. On the other hand, if we plot the thermoosmotic volume flux, J_v , against absolute temperature difference, ΔT , the values of $(\bar{s}_0 - s_0)$ can be directly obtained from the slope divided by osmotic coefficient, D^* .^{1,2,4,8} The difference was within 0.2% between the values of $(\bar{e}_0 - s_0 T_m)/T_m$ estimated from the slope of the plot of J_v against $\Delta \ln T$ and the values of $(\bar{s}_0 - s_0)$ estimated directly from the slope of the plot of J_v against ΔT . Therefore, we can conclude that the equation derived from a set of an entropy flux and the coupled absolute temperature difference force as dissipation function is a good approximation in the range of the small temperature difference ($\Delta T = \pm 10$ K) in this work. The transported energy and the mean transported entropy of water in the membrane, \bar{e}_0 and \bar{s}_0 , were estimated and values are also listed in Tables 2 and 3, assuming the partial molar entropy of water at 0.01 mol kg⁻¹ of electrolyte solutions equals 4.1 J K⁻¹ mol⁻¹ of the molar entropy of pure water at 308 K.⁹ In general, the values of $(\bar{e}_0 - s_0 T_m)$, $(\bar{s}_0 - s_0)$, \bar{e}_0 , and \bar{s}_0 increased with increasing the carbon number of alkyl groups, that is, the hydrophobicity of the membranes. It was concluded that the state of water in the membranes becomes unstable with increasing the hydrophobicity of the membranes.

Uedaira and Uedaira reported that water molecules in the immediate vicinity of nonpolar alkyl groups in tetraalkylamines became less mobile than in pure water due to the hydrophobic hydration between the alkyl chains and water.¹⁰

Yastremskii et al. also found that the stabilization of the water structure by the ions of the tetraalkylammonium salts is more effective, if the size of the alkyl groups in the dissolved salt is greater.¹¹ On the other hand, it was reported that, at higher concentrations of aqueous $(\text{C}_3\text{H}_7)_4\text{NBr}$ and $(\text{C}_4\text{H}_9)_4\text{NBr}$ solutions, the clathrate-like structure of water surrounding the cations would collapse because of the relatively small amount of water.¹² Moreover, it was shown that the destruction of the network structure of water surrounding the molecules of tetrabutylammonium hydroxide was increased by hydrophobic interactions at the higher concentrations, while the clear evidence of structural enhancement of the network was obtained in the dilute solutions due to the hydrophobic hydration.¹³ As shown in Table 1, the molalities of the fixed charges in the membranes were very high (3.7–6.7 mol kg⁻¹). The state of water in the membranes will be similar to that in the more concentrated alkylammonium solutions. For the more hydrophobic membranes such as M-5(10) and M-5(14), having benzyltripentylammonium the membranes act just as hydrophobic hydrocarbon membranes. In these cases the entropy difference, $(\bar{s}_0 - s_0)$, or the energy difference, $(\bar{e}_0 - s_0 T_m)$, becomes positive. Thermoosmosis across M-5(10), M-4(14), and M-5(14) appeared toward the cold side. This will be because the interfacial water structure near the hydrophobic surface is similar to that at the air–water interface¹⁴ and the state of water near the hydrophobic surface resembles that in the gas phase.¹⁵

Conclusions

1. The thermoosmotic volume flux toward the hot solution side decreased with increasing the length of alkyl groups (increasing hydrophobicity of the groups), and at last, for the membranes with benzyltripentylammonium, the direction of thermoosmosis reversed: from the hot to the cold solution side as is observed for usual hydrophobic membranes.
2. The transported energy and the mean transported entropy of water in the membrane estimated from the data of thermoosmosis and that of osmosis measurements increased with increasing the hydrophobicity of the ion-exchange groups introduced in the membranes.
3. The equation derived from a set of an entropy flux and the coupled absolute temperature difference force as dissipation function is a good approximation in the range of the small temperature differences ($\Delta T = \pm 10$ K).

References

- 1) M. Tasaka, T. Urata, R. Kiyono, and Y. Aki, *J. Membr. Sci.*, **67**, 83 (1992).
- 2) T. Suzuki, R. Kiyono, and M. Tasaka, *J. Membr. Sci.*, **92**, 85 (1994).
- 3) M. Tasaka, T. Suzuki, R. Kiyono, M. Hamada, and K. Yoshie, *J. Phys. Chem.*, **100**, 16361 (1996).
- 4) T. Suzuki, K. Iwano, R. Kiyono, and M. Tasaka, *Bull. Chem. Soc. Jpn.*, **68**, 493 (1995).
- 5) T. Sata, T. Yamaguchi, and K. Matsusaki, *J. Phys. Chem.*, **99**, 12875 (1995).
- 6) K. Bunzl and B. Sansoni, *Anal. Chem.*, **48**, 2279 (1976).

- 7) R. Kiyono, Y. Tanaka, O. Sekiguchi, and M. Tasaka, *Colloid Polym. Sci.*, **271**, 1183 (1993).
 - 8) M. Tasaka, Masud S. Huda, and R. Kiyono, *Bull. Chem. Soc. Jpn.*, **70**, 555 (1997).
 - 9) B. R. Lentz, A. T. Hagler, and H. A. Scheraga, *J. Phys. Chem.*, **78**, 1531 (1974).
 - 10) Hi. Uedaira and Ha. Uedaira, *Zh. Fiz. Khim.*, **42**, 3024 (1968).
 - 11) P. S. Yastremskii, G. V. Kokovina, A. K. Lyashchenko, and Yu. A. Mirgord, *Zh. Strukt. Khim.*, **16**, 1002 (1975).
 - 12) W.-Y. Wen and S. Saito, *J. Phys. Chem.*, **68**, 2639 (1964).
 - 13) J. L. Green, M. G. Sceats, and A. R. Lacey, *J. Chem. Phys.*, **87**, 3603 (1987).
 - 14) Q. Du, E. Freysz, and Y. R. Shen, *Science*, **264**, 826 (1994).
 - 15) H. Kusanagi, *Kobunshi: High Polym. Jpn.*, **42**, 314 (1993).
-